Universiteit Leiden
The Netherlands

Carbon starvation in the filamentous fungus Aspergillus niger

Nitsche, B.M.

Citation

Nitsche, B. M. (2012, October 23). *Carbon starvation in the filamentous fungus Aspergillus niger*. Retrieved from https://hdl.handle.net/1887/20011

Version:	Not Applicable (or Unknown)
License:	Leiden University Non-exclusive license
Downloaded from:	https://hdl.handle.net/1887/20011

Note: To cite this publication please use the final published version (if applicable).

Cover Page

Universiteit Leiden

Leiden University Repository

The handle http://hdl.handle.net/1887/20011 holds various files of this Leiden University dissertation.

Author: Nitsche, Benjamin Manuel
Title: Carbon starvation in the filamentous fungus Aspergillus niger
Date: 2012-10-23

Chapter 5

Autophagy promotes survival in aging submerged cultures of the filamentous fungus Aspergillus niger

Benjamin M. Nitsche[1,2,§], Anne-Marie van Welzen[1,3,§], Gerda Lamers[1,3], Vera Meyer[2,3], Arthur F.J. Ram[1,3]

[1]Institute of Biology, Leiden University, Sylviusweg 72, 2333 BE Leiden, The Netherlands
[2]Institute of Biotechnology, Berlin University of Technology, Gustav-Meyer-Allee 25, 13355 Berlin, Germany
[3]Kluyver Centre for Genomics of Industrial Fermentation, PO Box 5057, 2600 GA, Delft, The Netherlands
[§]Both authors equally contributed to the manuscript

Abstract

Autophagy is a well conserved catabolic process constitutively active in eukaryotes that is involved in maintaining cellular homeostasis by targeting of cytoplasmic content and organelles to vacuoles. Autophagy is strongly induced by limitation of nutrients including carbon, nitrogen and oxygen and is clearly associated with cell death. We previously demonstrated that the accumulation of empty hyphal compartments and cryptic growth in carbon starved submerged batch cultures of *A. niger* were accompanied by a joint transcriptional induction of autophagy genes. In this study we examined the role of autophagy by deleting the *atg*1, *atg*8 and *atg*17 orthologs in *A. niger* and phenotypically analyzing the deletion strains in surface and submerged cultures. Our results indicate that *atg*1 and *atg*8 are essential for efficient autophagy, whereas deletion of *atg*17 has little to no effect on autophagy. Depending on the kind of oxidative stress confronted with, autophagy deficiency renders *A. niger* either more resistant or more sensitive to oxidative stress. Fluorescence microscopy showed that mitochondrial turnover upon carbon depletion in submerged cultures is severely blocked in autophagy impaired mutants. Furthermore, automated image analysis demonstrated that autophagy promotes survival in maintained carbon starved cultures of *A. niger*. Taken together, our results suggest that besides its function in nutrient recycling, autophagy plays important roles in physiological adaptation by organelle turnover and protection against cell death upon carbon depletion in submerged cultures.

Submitted to Applied and Molecular Biotechnology

Introduction

The filamentous fungus *Aspergillus niger* is an important and versatile cell factory commonly exploited for the industrial-scale production of a wide range of enzymes and organic acids. Although numerous studies have been conducted aiming at improving our knowledge of degradative cellular activities that determine product yields in *A. niger* including secretion of proteases and the unfolded protein response (Peberdy, 1994; MacKenzie *et al.*, 2005; Jørgensen *et al.*, 2009; Mattern *et al.*, 1992; Braaksma *et al.*, 2009), the possible role of autophagy in relation to protein production has yet not been studied in this industrially important fungus.

Autophagy is an intracellular degradation process functioning in the delivery of cytoplasmic proteins and organelles to the vacuole for macromolecule turnover and recycling (Bartoszewska *et al.*, 2011b; Inoue *et al.*, 2010). During autophagy, cellular components are sequestered and transported to lytic compartments in double-membrane vesicles, termed autophagosomes. The outer membrane of the autophagosome fuses with the vacuolar membrane, whereupon a single membrane vesicle is released into the lumen. Following lysis of the autophagic membrane and degradation of its content by hydrolytic enzymes, the breakdown products are transported back into the cytoplasm for reuse by the cell.

The autophagy pathway is highly conserved from yeast to higher eukaryotes and is tightly regulated (Bartoszewska *et al.*, 2011b). To date, more than 30 autophagy-related (*atg*) genes have been identified for *Saccharomyces cerevisiae* and other fungi (Kanki *et al.*, 2011; Xie *et al.*, 2007). One key player controlling the levels of autophagy is the autophagy-related protein ATG1, which is a serine/threonine protein kinase (Bartoszewska *et al.*, 2011b; Inoue *et al.*, 2010). Upon induction of autophagy, this kinase interacts with ATG17, ATG29 and ATG31 in an ATG13-dependent manner, forming the ATG1-kinase complex and initiating the formation of autophagosomes (Cheong *et al.*, 2008; Kabeya *et al.*, 2005). Deletion of the *atg*1 ortholog in *Podospora anserina* abolished autophagy and caused several developmental defects (Pinan-Lucarré *et al.*, 2005). Mutants displayed fewer aerial hyphae and did not form protoperithecia. Similar phenotypic traits were observed in *P. anserina* $\Delta atg8$ mutants (Pinan-Lucarré *et al.*, 2005). ATG8 is coupled to the membrane lipid phosphatidylethanolamine (PE) forming an essential component of autophagic vesicle membranes (Bartoszewska *et al.*, 2011b; Inoue *et al.*, 2010). The *atg*8 gene has also been deleted in the filamentous fungus *Aspergillus oryzae*. The resulting mutants were defective in autophagy and formed no aerial hyphae and conidia (Kikuma *et al.*, 2006).

Autophagy plays an important role in cellular homeostasis by efficient removal of damaged organelles. For filamentous fungi it has been shown that endogenous recycling of cellular products by autophagy facilitates foraging of hyphae and fuels conidiation under nutrient starvation (Shoji *et al.*, 2006; Shoji *et al.*, 2011; Richie *et al.*, 2007). The hyphae that are formed

during this starvation-induced (cryptic) re-growth show fewer new branches and a significant decrease in hyphal diameter (Pollack *et al.*, 2008). In the older portions of the mycelium vacuolation increases dramatically following starvation, resulting in fragmentation and eventually dying of the hyphae.

We have shown previously that the morphological response to carbon starvation in submerged batch cultures of the filamentous fungus *A. niger*, including emergence of empty hyphal ghosts and thinner non-branching hyphae, is accompanied by the concerted induction of genes related to autophagy (Nitsche *et al.*, 2012a). To gain insights into the role of autophagy during submerged carbon starvation, *A. niger* autophagy mutants were generated by deletion of *atg*1, *atg*8 and *atg*17 gene orthologs. The mutants were phenotypically characterized during growth in surface and submerged cultures applying nutrient limitation and oxidative stress. Cytological effects of autophagy deficiency were assessed by investigation of fluorescent reporter strains allowing the visualization of cytoplasm, vacuoles and mitochondria. Our results indicate that autophagy plays important roles in metabolic adaptation to carbon starvation during submerged growth and thereby promotes the survival of pre-starvation formed hyphae.

Material and Methods

Strains, media and molecular techniques

Aspergillus strains used (Table 5.1) were grown at 30°C on solidified (20 $g \cdot l^{-1}$ agar) minimal medium (MM) (Alic *et al.*, 1991) or complete medium (CM) containing 0.5% (w/v) yeast extract and 0.1% (w/v) casamino acids in addition to MM. The pH of synthetic medium for bioreactor cultivations was adjusted to 3 and contained per liter: 4.5 g NH_4Cl, 1.5 g KH_2PO_4, 0.5 g KCl, 0.5 g $MgSO_4 \cdot 7H_2O$ and 1 ml trace metal solution (modified from Vishniac *et al.* (1957)). After autoclavation the synthetic media was supplemented with filter-sterilized 0.003% (w/v) yeast extract and 0.8% (w/v) glucose. Cloning was performed according to the methods described by Sambrook *et al.* (2001) using *Escherichia coli* strain DH5α. Transformation of *A. niger* was performed as described by Meyer *et al.* (2010). Hygromycin resistant transformants were isolated from plates supplemented with 200 $\mu g\ ml^{-1}$ hygromycin and 50 $\mu g\ ml^{-1}$ caffeine. MM for sensitivity plate assays was solidified with 2% (w/v) agar and supplemented with H_2O_2 or menadione as indicated.

Table 5.1 — Strains used

Strain	Genotype	Source
A. niger		
N402	*cspA1*	Bos *et al.* (1988)
AB4.1	*pyrG*$^-$	(Hartingsveldt *et al.*, 1987)
BN30.2	N402, $\Delta atg1$::hyg^R	this study
BN29.3	N402, $\Delta atg8$::hyg^R	this study
BN32.2	N402, $\Delta atg17$::hyg^R	this study
BN38.9	AB4.1, P*gpdA*::*N-citA*::*gfp*, *pyrG*$^+$	this study
BN39.2	BN38.9, $\Delta atg1$::hyg^R	this study
BN40.8	BN38.9, $\Delta atg8$::hyg^R	this study
AW20.10	BN38.9, $\Delta atg17$::hyg^R	this study
30.2 II	BN30.2, P*gpdA*::*gfp*, phl^R	this study
29.3 I	BN29.3, P*gpdA*::*gfp*, phl^R	this study
32.2 I	BN32.2, P*gpdA*::*gfp*, phl^R	this study
AR19#1	AB4.1, P*gpdA*::*gfp*, *pyrG*$^+$	Vinck *et al.* (2005)
A. nidulans		
SRS29	*pyrG*89, *pyroA*4, P*gpdA*::*NcitA*::*gfp*	Suelmann *et al.* (2000)

Construction of strains

The vector for constitutive expression of mitochondrially targeted GFP was constructed as follows. A 1.1 kb *NcitA*::*gfp* fragment was PCR amplified from genomic DNA of the *A. nidulans* strain SRS29 (Suelmann *et al.*, 2000), blunt-end ligated into pJET1.2 (Fermentas) and sequenced. Subsequently, the fragment was excised using *Bgl*II and *BamH*I and ligated into the 3.5 kb *Bgl*II-*BamH*I backbone of pAN52-1N (GenBank: Z32697.1). Next, a 2.2 kb *Bgl*II-*Nco*I *PgdpA* fragment from pAN52-1N was inserted into the *Bgl*II-*Nco*I opened intermediate construct. Finally, a 3.9 kb *Xba*I *pyrG** fragment was isolated from pAB94 (Gorcom *et al.*, 1988) and inserted at the *Xba*I site to give the final construct: *PgpdA-NcitA*::*gfp-TtrpC-pyrG**, which was transformed to *A. niger* strain AB4.1 (Hartingsveldt *et al.*, 1987). Single copy integration at the *pyrG* locus was confirmed by Southern analysis according to the method described by Meyer *et al.* (2010) (data not shown). The strain was named BN38.9.

Constructs for gene replacements with the hygromycin resistance cassette were generated as follows. Approximately 1 kb flanking regions of the *atg*1 (An04g03950), *atg*8 (An07g10020) and *atg*17 (An02g04820) open reading frames were PCR amplified from genomic DNA of the N402 wild-type strain using primer pairs according to Table 5.2, blunt-end ligated into pJET1.2 (Fermentas) and sequenced. Flanks were isolated from the pJET1.2 vectors using enzymes cutting at the outermost restriction sites (Table 5.2) and three-way ligated into a *Not*I-*Kpn*I opened pBluescript II SK(+) (Fermentas). For finalizing the *atg*1 and *atg*17 deletion constructs, the hygromycin resistance cassette was isolated as *Nhe*I-*Xba*I fragement and ligated between the flanking regions within the intermediate pBluescript constructs. For insertion of the hygromycin resistance cassette between the *atg*8 flanks, *Xho*I and *Xba*I were used. Linearized *atg*1, *atg*8 and *atg*17 deletion cassettes were transformed to *A. niger* strain N402 and homologous integration was confirmed by Southern analysis (data not shown) giv-

Table 5.2 — Primers used

Primer pairs (sequence 5' to 3' oriented)	Restriction site	Target
f: ataagaatgcggccgcATTAGTGAGTCGGTTGATGCCATG	*Not*I	5' flank *atg*1 (An04g03950)
r: ctagctagcttaatcctagtctagaGAGCGAAAGACAGGTCGGGA	*Nhe*I, *Xba*I	
f: ctagctagcCAGGCAACTGCATTCCAAGCTCG	*Nhe*I	3' flank *atg*1 (An04g03950)
r: cggggtaccGAATGACAAGCTACGGGTGAAAGA	*Kpn*I	
f: ataagaatgcggccgcGCCAGTAGTGGGTAGGGATTTGG	*Not*I	5' flank *atg*8 (An07g10020)
r: ccgctcgagttaatcctagtctagaGATAAGTAGATGAGGGCGGCTAG	*Xho*I, *Xba*I	
f: ccgctcgagGCGCTGGTCGATCTCCTCGTTTC	*Xho*I	3' flank *atg*8 (An07g10020)
r: cggggtaccGTGCAATCCAGGACCTGGACACAAA	*Kpn*I	
f: ataagaatgcggccgcGTGCTGCCAGTCTCGATTGG	*Not*I	5' flank *atg*17 (An02g04820)
r: ctagctagcttaatcctagtctagaGTCGGCGTAATTGGCGCTGA	*Nhe*I, *Xba*I	
f: ctagctagcTGCTCTGGTATTTCAGAGAGCTCG	*Nhe*I	3' flank *atg*17 (An02g04820)
r: cggggtaccGGTGATAATTGGGCTACTATGGGA	*Kpn*I	
f: ggaagatctcttggtttggtccATGGCTTCCACCTTGAGACTGG	*Bgl*II, *Nco*I	*NcitA* strain SRS29
r: cgcggatcccccaagtctaagcggccgcttacTTGTACAGCTCGTCCATGCCG	*BamH*I, *Not*I	*gfp* strain SRS29

f: forward strand; r: reverse strand; restriction sites are underlined

ing the stains BN30.2, BN29.3 and BN32.2, respectively (Table 5.1). For constitutive expression of cytosolically targeted GFP in atg mutants, the vector pGPDGFP (Lagopodi *et al.*, 2002) was co-transformed with pAN8.1 (Mattern *et al.*, 1988) to *A. niger* strains BN30.2, BN29.3 and BN32.2 (Table 5.1). Positive transformants were isolated by screening for cytosolic fluorescence and named 30.2 II, 29.3 I and 32.2 I, respectively (Table 5.1). Deletion of *atg*1, *atg*8 and *atg*17 in the strain expressing the mitochondria-targeted GFP was performed by transforming linearized *atg*1, *atg*8 and *atg*17 deletion constructs to *A. niger* strain BN38.9. Homologous integration of the constructs at their respective loci was confirmed by Southern analysis (data not shown) and the resulting strains were named BN39.2, BN40.8 and AW20.10, respectively (Table 5.1).

Bioreactor cultivation and sampling

Bioreactor cultivations were performed as previously described by Jørgensen *et al.* (2010). Briefly, autoclaved 6.6 L bioreactor vessels (BioFlo3000, New Brunswick Scientific) holding 5 L sterile synthetic medium were inoculated with $5 \cdot 10^9$ conidia. During cultivation, the temperature was set to 30°C and pH 3 was maintained by addition of titrants (2 M NaOH, 1 M HCl). The supply of sterile air was set to $1\ \mathrm{L} \cdot \mathrm{min}^{-1}$. To avoid loss of hydrophobic spores through the exhaust gas, the stirrer speed was set to 250 rpm and air was supplied via the head space during the first six hours of cultivation. After this initial germination phase, the stirrer speed was increased to 750 rpm, air was supplied via the sparger and 0.01% (v/v) polypropylene glycol (PPG) P2000 was added to prevent foaming. O_2 and CO_2 partial pressures of the exhaust gas were analyzed with a Xentra 4100C analyzer (Servomex BV, Netherlands). Dissolved oxygen tension (DOT) and pH were measured electrochemically with autoclavable sensors (Mettler

Toledo). At regular intervals, samples were taken from the cultures. Aliquots for microscopic analysis were either directly analyzed (fluorescence microscopy) or quickly frozen in liquid nitrogen (automated image analysis), the remainder of the samples was vacuum filtrated using glass microfiber filters (Whatmann). Retained biomass and filtrates were directly frozen in liquid nitrogen and stored at -80°C. Biomass concentrations were gravimetrically determined from freeze dried mycelium of a known mass of culture broth.

Microscopic and image analysis

For the analysis of hyphal diameters, microscopic samples were slowly defrosted on ice and subsequently fixed and stained in a single step by mixing them at a 1:1 ratio with Lactophenolblue solution (Fluka). Per sample, a minimum of 40 micrographs were taken using a 40x objective and an ICC50 camera (Leica). The microscope and camera settings were optimized to obtain micrographs with strong contrast. To measure hyphal diameters in an automated manner, a previously developed and described macro (Nitsche *et al.*, 2012a) for the open source program ImageJ (Abràmoff *et al.*, 2004) was used. DIC and fluorescence images were taken with a Zeiss axioplan 2 imaging microscope equipped with DIC optics. For the GFP settings, an epi-fluorescence filter cubeXF 100-2 with excitation 450-500 nm and emission 510-560 nm was used. Confocal images were obtained using a Zeiss Observer microscope coupled to a LSM 5 exciter. Excitation in the GFP settings was achieved with a 488 Argon laser line with emission 505-550 nm.

Results

Autophagy-related genes *atg*1 and *atg*8 but not *atg*17 are essential for efficient autophagy in *A. niger*

To study the phenotypes of autophagy deficient *A. niger* mutants in surface and submerged cultures, we identified and deleted orthologs of three genes known to encode essential components of the autophagic machinery in *S. cerevisae* (Tsukada *et al.*, 1993; Matsuura *et al.*, 1997; Cheong *et al.*, 2005; Kabeya *et al.*, 2005). Two of the target genes encode proteins that are part of the regulatory ATG1 kinase complex, namely the kinase ATG1 itself and the scaffold protein ATG17. The third target gene encodes the ubiquitin-like protein ATG8, which is a structural component required for the formation of autophagosomal membranes. We identified the following ortholog pairs *Scatg*1/An04g03950 ($E = 4e^{-151}$), *Scatg*8/An07g10020 ($E = 4e^{-67}$) and *Scatg*17/An02g04820 ($E = 2e^{-12}$) by reciprocal best BlastP hit analysis and subsequently deleted these target genes in the *A. niger* laboratory wild-type strain N402 by replacement with a

hygromycin resistance cassette. Gene deletions were confirmed by Southern analysis (data not shown).

Previous studies in *A. oryzae* (Kikuma *et al.*, 2006) and *Penicillium chrysogenum* (Bartoszewska *et al.*, 2011a) demonstrated localization of cytosolic fluorescent protein to vacuoles under starvation conditions in wild-type strains, whereas mutants impaired in autophagy did not show vacuolar localization of cytosolic GFP. Therefore we generated $\Delta atg1$, $\Delta atg8$ and $\Delta atg17$ strains in a background with constitutive expression of cytosolic GFP to assess whether deletion of the respective *atg* genes impairs autophagy in *A. niger*. Vacuolar localization of cytosolic GFP was observed for the wild-type strain during nutrient limitation, while both $\Delta atg1$ and $\Delta atg8$ mutants did not show GFP fluorescence inside vacuoles, indicating deficient autophagy. Interestingly, deletion of *atg17* did not affect vacuolar localization of cytosolic GFP (see Figure 5.1). These results suggest that both $atg1$ and $atg8$ but not $atg17$ are essential for efficient autophagy in *A. niger*.

In order to monitor autophagy dependent turnover of mitochondria (mitophagy) (Kanki *et al.*, 2011) induced by carbon starvation, we generated wild-type and atg mutant strains with constitutive expression of mitochondrially targeted GFP. We used the same approach to vi-

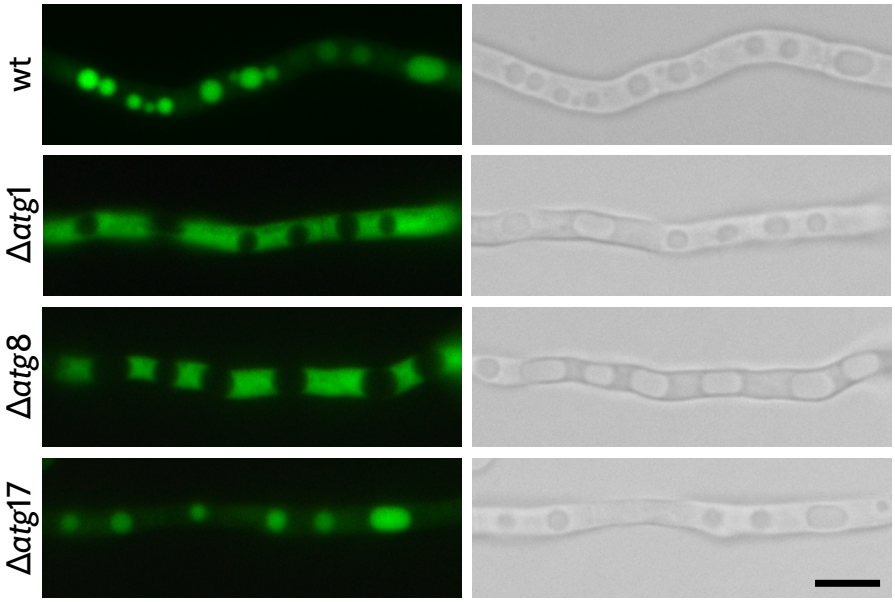

Figure 5.1 – Localization of cytosolically expressed GFP during carbon starvation
The strains were pregrown for 8 hours at 30°C on coverslips in Petri dishes with liquid MM. Subsequently coverslips with adherent hyphae were washed and transferred to MM without carbon source. Micrographs were taken 40 hours after transfer. Wild-type and $\Delta atg17$ mutant showed vacuolar localization of GFP, whereas both $\Delta atg1$ and $\Delta atg8$ mutants showed cytosolic localization. Scale bar: 5 μm

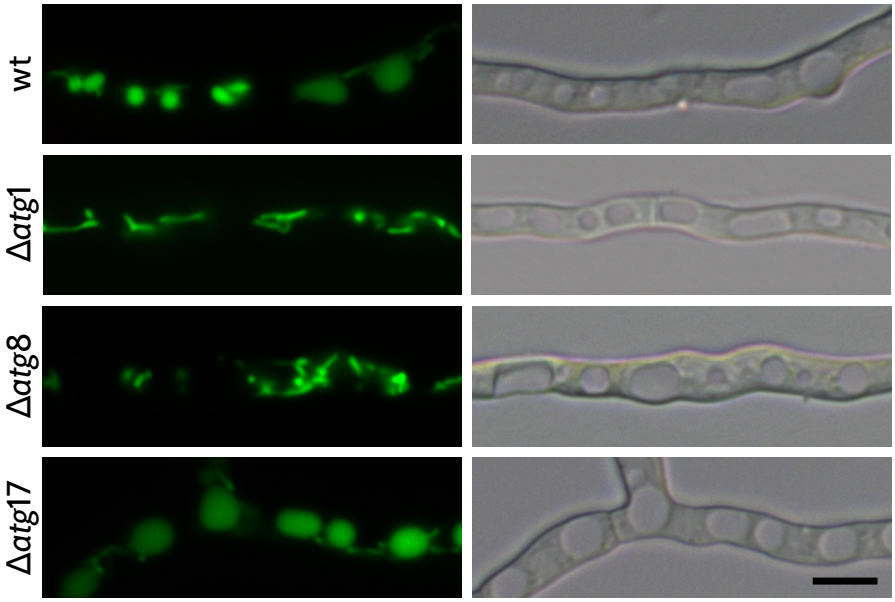

Figure 5.2 – Localization of mitochondrially expressed GFP during carbon starvation
The strains were grown as described in Figure 5.1. Wild-type and Δ*atg*17 mutant showed vacuolar localization of GFP, whereas both Δ*atg*1 and Δ*atg*8 mutants showed mitochondrial localization. Under nutrient-rich conditions, all strains showed fluorescent patterns resembling tubular mitochondrial networks as previously shown by Suelmann *et al.* (2000). Scale bar: 5 μm

sualize mitochondria as described by Suelmann *et al.* (2000), who showed that N-terminal fusion of the mitochondrial targeting sequence from the citrate synthase A to a fluorescent protein efficiently labeled mitochondria. For wild-type and mutant reporter strains, exponentially growing hyphae showed fluorescent tubular structures resembling those described by Suelmann *et al.* (Figure 5.6). During carbon starvation however, microscopic analysis of those mitochondrial reporter strains indicated considerable differences in mitochondrial turnover between wild-type and atg mutants (Figure 5.2). The differences correspond to those observed for the localization of cytosolic GFP (Figure 5.1). The localization of GFP remained mitochondrial in both $\Delta atg1$ and $\Delta atg8$ mutant strains, whereas wild-type and $\Delta atg17$ strains showed vacuolar localization of mitochondrially expressed GFP. Thus suggesting that mitochondrial turnover induced by carbon starvation is mediated by autophagy, which is severely impaired in the $\Delta atg1$ and $\Delta atg8$ mutants.

Phenotypes of Δ*atg*1, Δ*atg*8 and Δ*atg*17 strains in surface cultures

Depending on which species of filamentous fungi is studied and which *atg* gene is under investigation, defective autophagy results in complete or severe impairment of conidiation during surface growth (Richie *et al.*, 2007; Bartoszewska *et al.*, 2011a; Kikuma *et al.*, 2006). To test whether conidiation in *A. niger* atg mutants is affected as well, we harvested and counted conidia from colonies grown for 7 days on solid MM. Although colonies of the Δ*atg*1 and Δ*atg*8 mutants developed conidiophores and turned dark, the colonies showed slightly attenuated pigmentation (see Figure 5.3A) indicating reduced spore densities and/or differences in melanization of spores. Indeed, the number of spores recovered from the Δ*atg*1 and Δ*atg*8 colonies were significantly reduced (see Figure 5.3C). With a decrease of 70%, conidiation was most affected in the Δ*atg*8 mutant. Interestingly, although the Δ*atg*17 mutant showed vacuolar localization of cytosolic (Figure 5.1) and mitochondrial (Figure 5.2) GFP under carbon starvation and its colony appearance was indistinguishable from that of the wild-type, the number of recovered conidia was reduced by 20%, thus suggesting an intermediate phenotype of the Δ*atg*17 mutant. In agreement to studies in *A. oryzae* (Kikuma *et al.*, 2006) the Δ*atg*8 strain showed slower radial growth on synthetic medium (see Figure 5.3B). However, even considering the differences in colony sizes, conidiation was most reduced for the Δ*atg*8 mutant as shown by the spore densities (see Figure 5.3C). Compared to the *A. oryzae* Δ*atg*8 mutant, which was reported not to develop aerial hyphae and conidia (Kikuma *et al.*, 2006), the conidiation phenotype in *A. niger* is much less pronounced.

In filamentous fungi, autophagy has been suggested to contribute to nutrient recycling along the mycelial network promoting foraging of individual substrate exploring hyphae and conidial development (Richie *et al.*, 2007; Shoji *et al.*, 2006; Shoji *et al.*, 2011). We have investigated the phenotypes of the mutants during nitrogen and carbon limitation on solid MM (see Figure 5.4A). The Δ*atg*1 and Δ*atg*8 mutants were clearly more affected by nutrient limitation than the wild-type as shown by their strong conidiation phenotypes. Whereas the mutants were comparably affected by carbon limitation, the Δ*atg*8 mutant was more sensitive to nitrogen limitation than the Δ*atg*1 mutant. In accordance with results presented in Figures 5.1, 5.2 and 5.3A, the phenotype of the Δ*atg*17 mutant during nitrogen and carbon limitation is indistinguishable from that of the wild-type.

In addition to its role in nutrient recycling, numerous reports have shown that autophagy is closely associated with Programmed Cell Death (PCD) (Pinan-Lucarré *et al.*, 2005; Veneault-Fourrey *et al.*, 2006; Codogno *et al.*, 2005). Major triggers of PCD are reactive oxygen species (ROS) and the damage they can cause to lipids, carbohydrates, DNA and proteins. We were interested in oxidative stress related phenotypes of the autophagy mutants and performed sensitivity assays with H_2O_2 and the superoxide anion generator menadione (see Figure 5.4B-C)

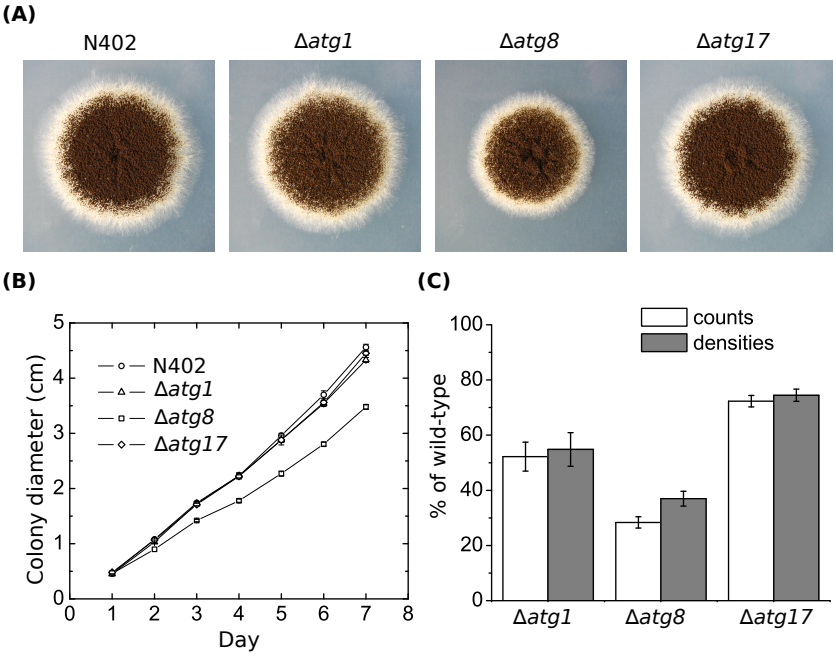

Figure 5.3 — Phenotypes of wild-type and atg mutants.
Strains were grown for seven days on solid MM at 30°C. (A) Colony appearance. (B) Colony diameters (n = 3). (C) Recovered conidia (n = 3).

which were shown to cause distinct oxidative stress responses in yeast and filamentous fungi (Thorpe *et al.*, 2004; Tucker *et al.*, 2004; Jamieson, 1992; Pócsi *et al.*, 2005). In comparison to the wild-type, the mutants displayed differential phenotypes in response to treatment with the two compounds. Interestingly, H_2O_2 and menadione had opposing effects. The mutants were more sensitive to H_2O_2, while their resistance to menadione was increased. The $\Delta atg17$ mutant displayed an intermediate phenotype, which was more comparable to that of the wild-type.

Taken together the phenotypic characterization suggests that autophagy is severely impaired in the $\Delta atg1$ and $\Delta atg8$ mutants. Contrary to this, the $\Delta atg17$ mutant showed little to no phenotypic differences when compared to the wild-type. The subsequent analysis of autophagy impairment during submerged cultivation was therefore restricted to the investigation of $\Delta atg1$ and $\Delta atg8$ mutants.

Phenotypes of Δ*atg*1 and Δ*atg*8 strains during submerged growth

We have previously demonstrated that the majority of the autophagy genes show joint induction after exponential growth in carbon-limited submerged batch cultures of *A. niger*. Concomitantly, old hyphae grown during the exponential phase underwent cell death resulting in an increased fraction of empty hyphal compartments and secondary (cryptic) growth of thin non-branching hyphae (Nitsche *et al.*, 2012a). Although it has been shown for filamentous fungi that autophagy plays an important role in nutrient recycling during surface growth (Richie *et al.*, 2007; Shoji *et al.*, 2006; Shoji *et al.*, 2011), its function in submerged cultures remains obscure. To gain insights into the role of autophagy during submerged carbon star-

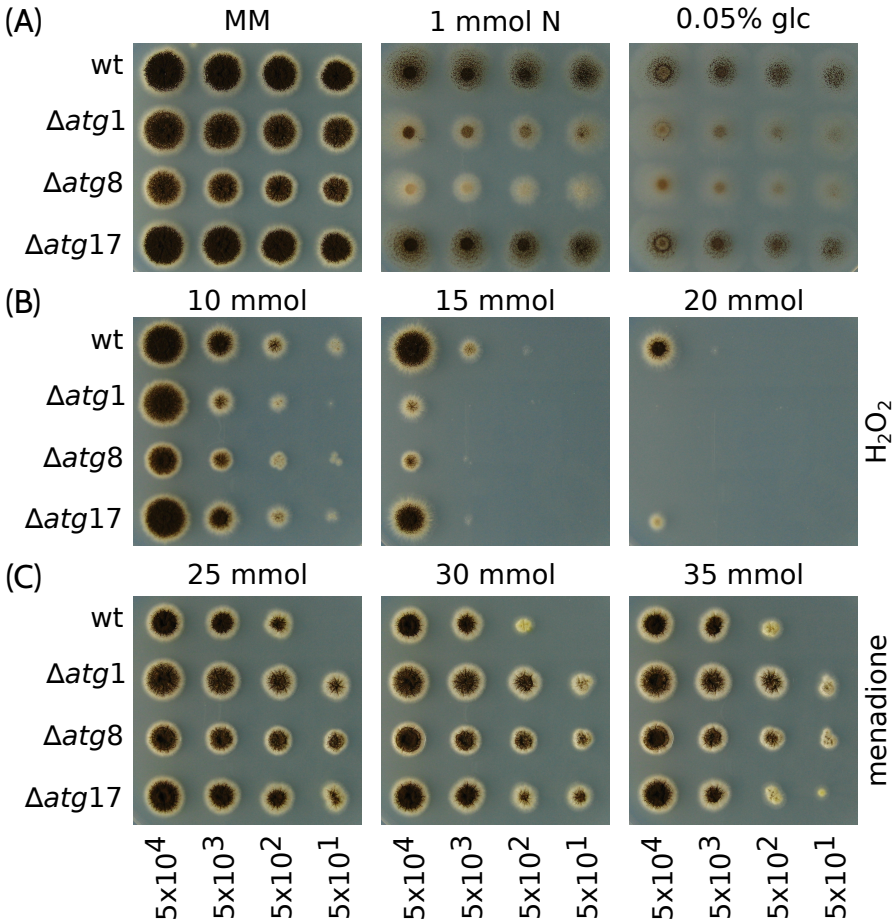

Figure 5.4 – Sensitivity assay of wild-type and atg mutants
10-fold dilutions ($5 \cdot 10^4$ - $5 \cdot 10^1$ conidia) were spotted on plates with (A) MM and MM with N (nitrate) or C (glucose) limitation, MM supplemented with (B) H_2O_2 or (C) menadione. Plates were incubated for 4 days at 30°C.

vation and to investigate how autophagy is related to the phenomena of cell death and secondary growth, we grew the $\Delta atg1$ and $\Delta atg8$ mutants in bioreactors and maintained the cultures starving up to six days after carbon depletion (Figure 5.5). Bioreactor cultivations were reproducible and monitoring of physiological parameters (DOT, off-gas and titrant addition) allowed synchronization of cultures. The described cultivation conditions prevented the formation of mycelial aggregates (pellets) and guaranteed a dispersed macromorphology during all cultivations. Interestingly, in contrast to the colony expansion rate on solid media (Figure 5.3A-B), the maximum specific growth rates for both mutants during exponential growth were affected to the same extend during submerged cultivation. Both mutants grew slower ($\mu_{\max} = 0.22\text{h}^{-1} \pm 0.005$) than the wild-type ($\mu_{\max} = 0.27\text{h}^{-1} \pm 0.021$). Considering the reproducibility of replicate cultures, the biomass profiles did not show any significant differences during the post-exponential phase (see Figure 5.5).

It was shown that autophagy is important for mitochondrial maintenance and degradation of excess mitochondria during the stationary phase of *S. cerevisiae* cultures, which is of outermost importance because mitochondria play a key role in metabolism and cell death

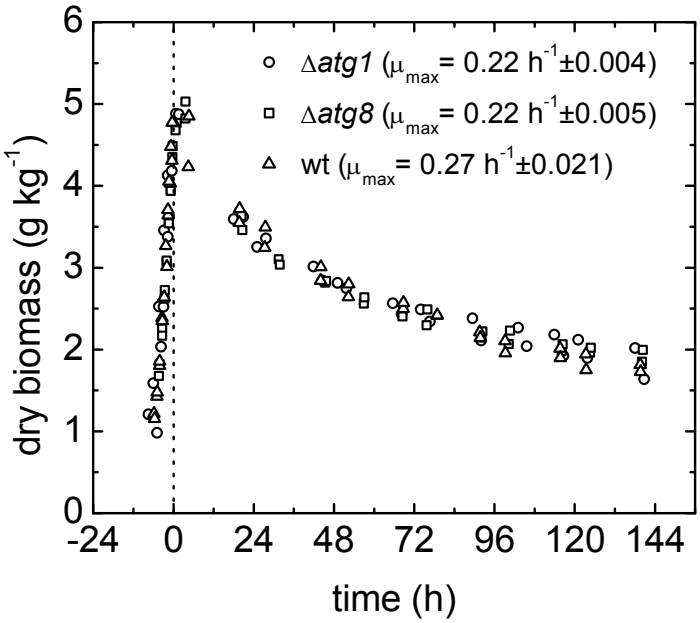

Figure 5.5 – Growth curves of carbon-limited submerged batch cultures
Growth curves for carbon-limited batch cultures of wild-type, $\Delta atg1$ and $\Delta atg8$ mutants. The time point of carbon depletion was set to 0 hours and used to synchronize replicate cultures.

signaling (Zhang *et al.*, 2007). We thus examined the morphology and degradation of mitochondria in *A. niger* wild-type, $\Delta atg1$ and $\Delta atg8$ strains during carbon starvation in bioreactor batch cultures by fluorescence microscopy of strains which constitutively express mitochondrially targeted GFP. Analysis of hyphae from the exponential growth phase showed fluorescent tubular structures resembling those described by Suelmann *et al.* (2000) and no difference in mitochondrial morphology was observed between the wild-type and the two mutants (Figure 5.6A). However, clear differences became apparent upon depletion of the carbon source. The mitochondrially targeted GFP was located inside the vacuoles in the wild-type background, whereas no vacuolar GFP signal was detected for both $\Delta atg1$ and $\Delta atg8$ mutants (Figure 5.6B-C). The density of mitochondrial structures decreased in the wild-type hyphae but accumulated in the space between vacuoles in the mutants. There were also considerable differences in the mitochondrial morphology. Remaining mitochondrial structures were largely tubular in the wild-type, while they appeared as fragmented and punctuated structures in the mutants.

In flow chamber experiments with *A. oryzae* Pollack *et al.* (2008) showed that carbon depletion induces outgrowth of hyphae with strongly reduced diameters. We previously observed a similar morphological response during carbon starvation in submerged cultures of *A. niger* (Nitsche *et al.*, 2012a). Hyphal population dynamics for the cytoplasm filled mycelial fraction demonstrated a gradual transition from thick (old) to thin (young) hyphae during the post-exponential phase which reflects cell death resulting in the emergence of empty thick compartments fueling secondary regrowth in the form of elongating thin hyphae. To examine whether autophagy affects this transition dynamic, we analyzed microscopic pictures of wild-type and both $\Delta atg1$ and $\Delta atg8$ mutant cultures. During exponential growth (day 0) all three strains displayed single populations of thick hype with mean diameters of approximately 2.2 μm. After carbon depletion, populations of thin hyphae with mean diameters of around 1 μm emerged. While this transition was gradual for the wild-type, it was clearly accelerated for the $\Delta atg1$ and $\Delta atg8$ mutants suggesting enhanced cell death rates for the older (thick) hyphae (Figure 5.7).

Discussion

To our knowledge, this is the first study of autophagy in the industrially important filamentous fungus *A. niger*. Improving our understanding of this catabolic pathway and its role during submerged cultivation is of great interest because autophagy has been shown to be involved in endogenous recycling and the regulation of cell death, both of which can have a direct impact on the yield of bioprocesses (Bartoszewska *et al.*, 2011b; Zustiak *et al.*, 2008). For different fil-

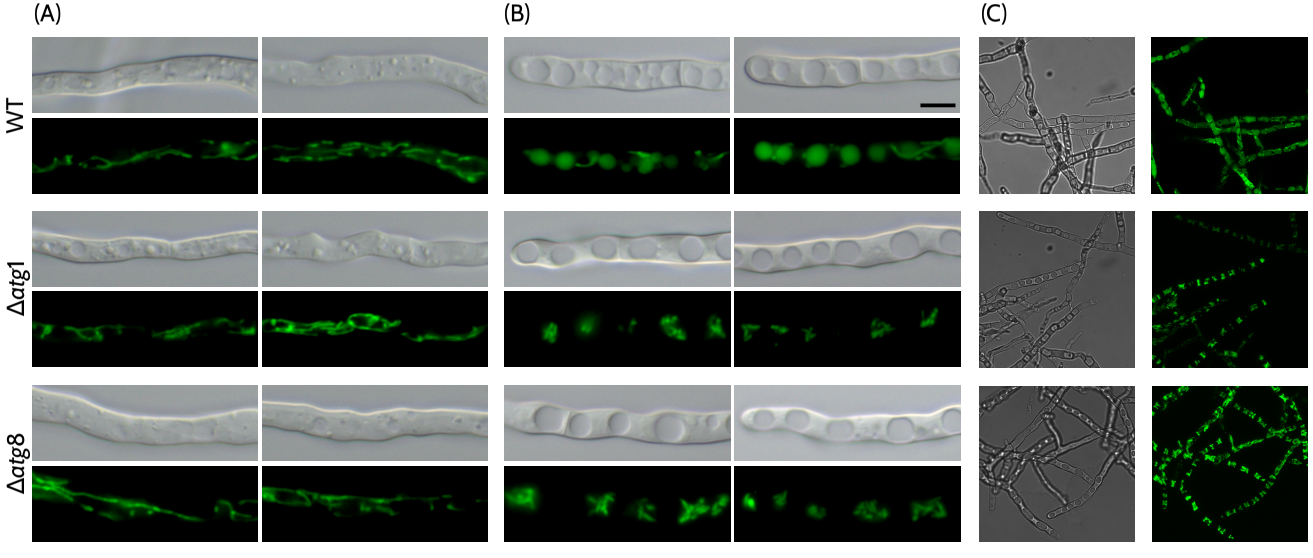

Figure 5.6 – Localization of mitochondrially expressed GFP during batch cultivation
Constitutive expression of mitochondrially targeted GFP in wild-type, Δ*atg*1 and Δ*atg*8 mutants during carbon-limited batch cultures. Differential interference contrast and fluorescence microscopy of hyphae from the exponential growth phase (A) and 7 hours post-carbon depletion (B). Confocal laser scanning microscopy of mycelial biomass at 14 hours post-carbon depletion (C). Scale bar: 5 μm.

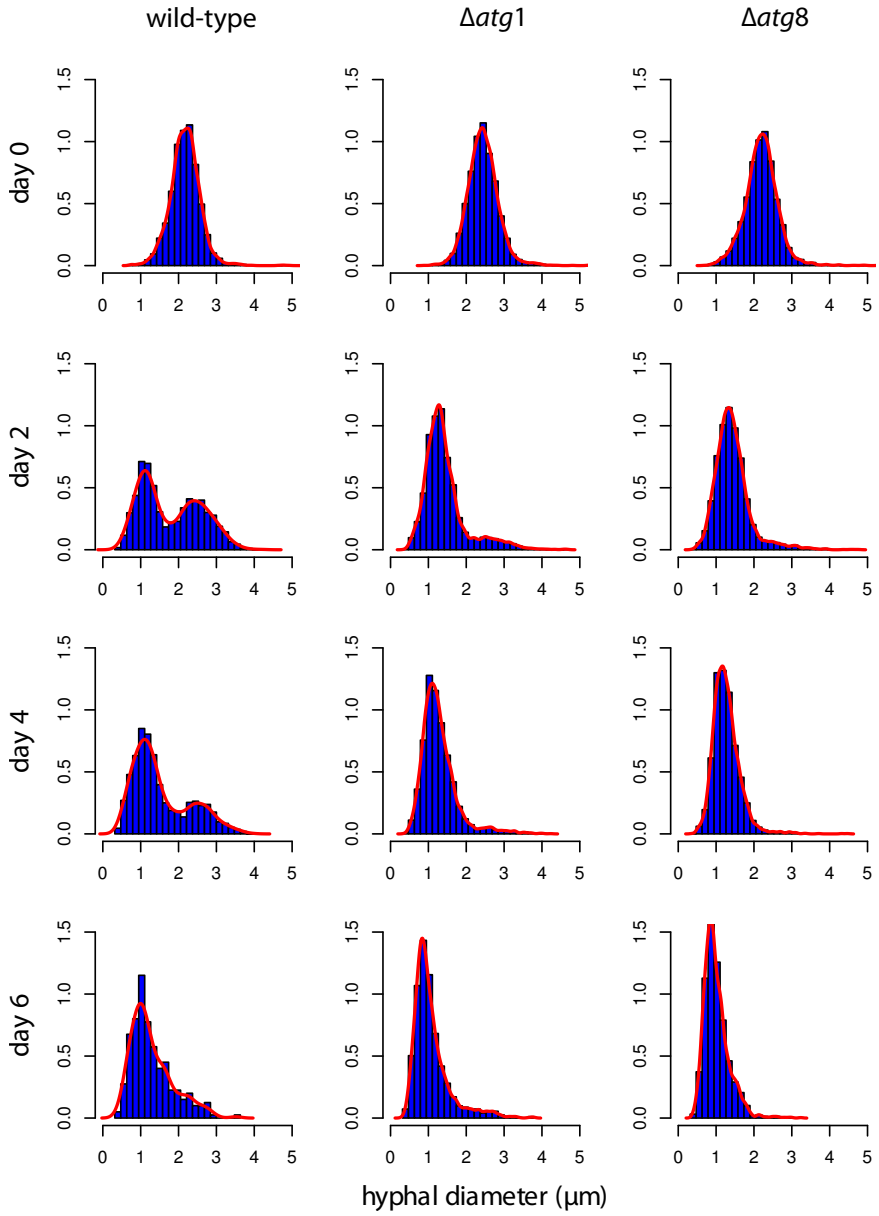

Figure 5.7 – Hyphal diameter populations
Population dynamics of hyphal diameters for wild-type, Δ*atg*1 and Δ*atg*8 mutants. ≥ 40 micrographs of dispersed hyphae were analyzed per strain and time point as described in the materials and methods sections.

amentous fungi, several studies analyzed phenomena of carbon starved submerged cultures (White *et al.*, 2002; Emri *et al.*, 2004; Emri *et al.*, 2005b; Emri *et al.*, 2006). The generic term that has emerged in this context is autolysis. It has been generally used to describe hallmarks of aging cultures including biomass decline, increasing extracellular ammonia concentration, hyphal fragmentation and increasing extracellular hydrolase activities (White *et al.*, 2002). Considerable effort has been made to analyze extracellular hydrolase activities (McNeil *et al.*, 1998; McIntyre *et al.*, 2000; Emri *et al.*, 2005b) as well as developmental mutants differentially affected in aging carbon starved cultures (Emri *et al.*, 2005b). However, the role of autophagy in those cultures has not attained much attention yet. In a recent systems level analysis of the *A. niger* transcriptome during submerged carbon starvation, we identified autophagy as a predominantly induced key process (Nitsche *et al.*, 2012a). In this present study, we thus aimed at elucidating whether autophagy protects from or promotes loss of hyphal integrity, which was mainly observed by the formation of empty hyphal ghosts.

In order to study autophagy deficiency in *A. niger*, we deleted two genes encoding components of the regulatory ATG1 kinase complex, namely the genes highly homologous to the kinase ATG1 itself and the scaffold protein ATG17. In addition, we deleted the $atg8$ gene encoding a membrane protein required for autophagosome formation and extension. In agreement to studies in yeast and other filamentous fungi (Bartoszewska *et al.*, 2011b), our results demonstrate that the deletion of either $atg1$ or $atg8$ is sufficient to severely impair autophagy in *A. niger*. However, conflicting with results obtained in *S. cerevisiae* (Cheong *et al.*, 2005; Kabeya *et al.*, 2005), where the absence of ATG17 severely reduces the level of autophagy, we were not able to demonstrate that autophagy is considerably impaired in the *A. niger* $\Delta atg17$ mutant. Similarly, the deletion of $atg13$ in *A. oryzae* encoding another subunit of the ATG1 kinase complex was reported to only gently affect autophagy, whereas deletion of its counterpart in *S. cerevisiae* clearly impaired it (Kikuma *et al.*, 2011). The authors suggested that ATG13 acts as an amplifier resulting in higher autophagic activities in *A. oryzae*. Probably, ATG17 has a similar enhancing role during autophagy induction in *A. niger* leading to the intermediate phenotypes described in this study.

Endogenous recycling of nutrients by autophagy has been supposed to be an important mechanism for nutrient trafficking along the mycelial network promoting foraging of substrate exploring filaments and the formation of aerial hyphae bearing conidiophores (Shoji *et al.*, 2006; Shoji *et al.*, 2011; Richie *et al.*, 2007). Similar to studies in other filamentous fungi (Richie *et al.*, 2007; Bartoszewska *et al.*, 2011a; Kikuma *et al.*, 2006), impairment of autophagy in *A. niger* considerably reduced conidiation (Figure 5.3), a phenotype, which was much enhanced by more severe carbon and nitrogen starvation conditions (Figure 5.4A).

In addition to its role in nutrient recycling, autophagy has been shown to be associated with PCD, which is classically categorized into three types, namely apoptotic (type I), autophagic (type II) and necrotic (type III) cell death. Although autophagy is also referred to as type II programmed cell death, it is not explicitly causative to cell death. Depending on the organism, cell type and stressor, autophagy has been shown to promote both cell death and survival. In filamentous fungi, it has for example been demonstrated to protect against cell death during the heterokaryon incompatibility reaction in *Podospora anserina* (Pinan-Lucarré *et al.*, 2005) or during carbon starvation in *Ustilago maydes* (Nadal *et al.*, 2010). Contrary to this, autophagy induced cell death is for example required for rice plant infection by *Magnaporthe grisea* (Veneault-Fourrey *et al.*, 2006). Loss of cellular integrity and subsequent death induced by damage of organelles, macromolecules and membranes through reactive oxygen species is a major threat for aerobic organisms. Well described enzymatic and non-enzymatic defense systems have evolved that detoxify ROS (Bai *et al.*, 2003). Autophagy is one of the major pathways for turnover of redundant or damaged organelles and proteins. The hypersensitivity of autophagy mutants to H_2O_2 thus fits our expectation and could be explained by an impaired capability of the mutants to sequester and degrade proteins and organelles damaged by H_2O_2. Increased resistance to menadione however, was unexpected but might be related to an adaptive stress response in autophagy deficient mutants. In *S. cerevisiae* it was for example shown that disruption of essential ATG genes results in increased oxidative stress and superoxide dismutase activities (Zhang *et al.*, 2007). Adaptive responses to oxidative stress induced by sublethal concentrations of exogenous oxidants have been demonstrated to protect yeast cells against higher lethal concentrations (Jamieson, 1992; Fernandes *et al.*, 2007). However, future studies will be required to elucidate the adaptive mechanism leading to menadione resistance in autophagy deficient mutants.

Hyphal population dynamics showed that the transition from old (thick) to young (thin) hyphae in response to carbon starvation during submerged cultivation was accelerated for both $\Delta atg1$ and $\Delta atg8$ mutants when compared to the wild-type (Figure 5.7). These results suggest that autophagy delays cell death of old hyphae under carbon starvation. Similar to a study with yeast (Suzuki *et al.*, 2011), fluorescence microscopy of wild-type, $\Delta atg1$ and $\Delta atg8$ reporter strains with GFP-labeled mitochondria revealed that degradation of mitochondria in response to carbon depletion is impaired in autophagy deficient mutants. The degradation of excess mitochondria during the stationary phase constitutes a physiological adaptation to the reduced energy requirement of the cells (Kanki *et al.*, 2011). It is tempting to speculate that autophagy impairment leads to increasing cellular ROS levels caused by the accumulation of excessive and damaged mitochondria, subsequently leading to loss of cellular integrity and finally the emergence of empty hyphal compartments. Taken together, the results indicate that the in-

duction of autophagy is not only required for endogenous recycling but also for physiological adaptation to carbon starvation by turnover of excessive organelles.

Acknowledgments

This work was supported by grants of the SenterNovem IOP Genomics project (IGE07008). Part of this project was carried out within the research programme of the Kluyver Centre for Genomics of Industrial Fermentation, which is part of the Netherlands Genomics Initiative / Netherlands Organization for Scientific Research. This work was (co)financed by the Netherlands Consortium for Systems Biology (NCSB) which is part of the Netherlands Genomics Initiative / Netherlands Organisation for Scientific Research. We thank Reinhard Fischer from the Karlsruhe Institute of Technology in Germany for providing us with the strain SRS29. We thank Crescel Martis and Leonie Schmerfeld for technical assistance.